Neuronal cell lines as model dorsal root ganglion neurons: A transcriptomic comparison

Kathleen Yin, BPharm[1,2], Gregory J Baillie, PhD[1] and Irina Vetter, PhD[1,2]

Abstract

Background: Dorsal root ganglion neuron-derived immortal cell lines including ND7/23 and F-11 cells have been used extensively as *in vitro* model systems of native peripheral sensory neurons. However, while it is clear that some sensory neuron-specific receptors and ion channels are present in these cell lines, a systematic comparison of the molecular targets expressed by these cell lines with those expressed in intact peripheral neurons is lacking.

Results: In this study, we examined the expression of RNA transcripts in the human neuroblastoma-derived cell line, SH-SY5Y, and two dorsal root ganglion hybridoma cell lines, F-11 and ND7/23, using Illumina next-generation sequencing, and compared the results with native whole murine dorsal root ganglions. The gene expression profiles of these three cell lines did not resemble any specific defined dorsal root ganglion subclass. The cell lines lacked many markers for nociceptive sensory neurons, such as the *Transient receptor potential V1* gene, but expressed markers for both myelinated and unmyelinated neurons. Global gene ontology analysis on whole dorsal root ganglions and cell lines showed similar enrichment of biological process terms across all samples.

Conclusions: This paper provides insights into the receptor repertoire expressed in common dorsal root ganglion neuron-derived cell lines compared with whole murine dorsal root ganglions, and illustrates the limits and potentials of these cell lines as tools for neuropharmacological exploration.

Background

Peripheral sensory neurons enable humans to sense the world around us. Sensory nerve endings innervating the skin, muscle, and viscera are responsible for detecting external stimuli such as touch, vibration, temperature, and pain, which are then relayed to the spinal cord and the central nervous system. Peripheral sensory neurons are a heterogeneous group of neurons that can be classified according to axonal transmission speed, degrees of myelination, and functional characteristics.[1] The cell bodies of these pseudo-unipolar neurons are located in the dorsal root ganglia (DRG) and are used extensively to study mammalian sensory processes, peripheral mechanisms of pain, and the effect of drugs on the peripheral nervous system. In recent years, significant advances have been made in unravelling the molecular and pharmacological basis of the diverse functional properties defining subsets of peripheral sensory neurons, as well as the G-protein coupled receptors (GPCRs) and ion channels contributing to sensory neuron physiology and pathophysiology. For example, the transient receptor potential (TRP) channels including TRPV1, TRPA1, and TRPM8 are activated by temperature and reactive chemicals, while GPCRs such as protease-activated

[1]Centre for Pain Research, Institute for Molecular Bioscience, University of Queensland, Queensland, Australia
[2]Pharmacy Australia Centre of Excellence, University of Queensland, Queensland, Australia

Corresponding author:
Irina Vetter, Centre for Pain Research, Institute for Molecular Bioscience, 306 Carmody Road, Building 80, University of Queensland, St Lucia, Queensland 4072, Australia.
Email: i.vetter@uq.edu.au

receptors, histamine receptors, and bradykinin receptors are activated by inflammatory mediators. While primary DRG neurons are used extensively to study the pharmacological mechanisms involved in sensory neuron functions such as pain and itch, this approach has several drawbacks. The isolation and culture of DRG neurons is time consuming, highly technical, and requires the use of animals. Importantly, not all neurons survive this process.[2] Removal of DRG neurons from the *in vivo* environment and axotomy of the peripheral processes also leads to adaptive changes such as down-regulation of the potassium channel subunit $K_V9.1$, overexpression of the nerve growth factor receptor TrkA, and increased neuronal excitability.[3–6] In addition, as DRG neurons are heterogeneous, only a subset of cells is likely to express the target of interest and a substantial proportion of cultured cells include non-neuronal cell types such as fibroblasts and glial cells. Accordingly, researchers have turned to DRG-derived immortal cell lines as substitutes for intact DRG neurons when investigating endogenous receptors. Common candidates are the DRG-hybridoma cell lines F-11 and ND7/23, which were derived from embryonic or neonatal rat DRG neurons by fusion with the mouse neuroblastoma cell line N18Tg2[7,8] and display neuron-like properties including excitable membranes and sensory neuronal cell surface markers. Similarly, we have recently shown that the neuroblastoma cell line SH-SY5Y, which is commonly used as a model of adrenergic or dopaminergic neurons, exhibits traits of peripheral sensory neurons such as functional expression of the sensory neuron-specific sodium channel isoform $Na_V1.7$.[9] However, although these cell lines are often considered suitable models to study mechanisms of nociceptor activation and individual investigations of specific protein families have been conducted,[9–11] a systematic analysis of the expression profile of these cell lines in comparison with DRG neurons is lacking.

In this study, we conducted RNA-Seq analysis with particular emphasis on ion channel and GPCR expression in DRG neuron-derived cell lines including the human neuroblastoma cells SH-SY5Y,[12,13] the mouse neuroblastoma/rat embryonic DRG neuron hybrid cell line F-11,[8] and the mouse neuroblastoma/rat neonatal DRG neuron hybrid cell line ND7/23.[7] Data from cell lines were then compared to RNA-Seq analysis conducted on whole murine DRG. Functional expression of selected targets was confirmed by Ca^{2+} imaging. While a number of sensory neuron-specific targets including $Na_V1.7$ were expressed in all cell lines, we also found several discrepancies, and none of the cell lines displayed an expression profile consistent with specific subclasses of sensory neurons. This stresses the need for further exploration on the functional receptors present on neuronal cell lines used as model DRG neurons, and highlights the importance for cautious interpretation of results obtained using SH-SY5Y, F-11, and ND7/23 cells.

Methods

Animals

Male wild-type C57BL/6 mice age six to eight weeks and weighing 20–23 g were used in the study. Ethical approval for experiments involving animal tissues was obtained from the University of Queensland animal ethics committee. Experiments were conducted in accordance with the Animal Care and Protection Regulation Qld (2012), the Australian Code of Practice for the Care and Use of Animals for Scientific Purposes, 8th edition (2013), and the International Association for the Study of Pain Guidelines for the Use of Animals in Research. All animals were obtained from University of Queensland Biological Resources (Brisbane, Australia).

Chemicals

The following compounds were obtained from Life Technologies (Mulgrave, Victoria, Australia): L-glutamine, Dulbecco's Modified Eagle Medium (DMEM), Ham's F12 media, Roswell Park Memorial Institute medium, 0.25% trypsin/EDTA, foetal bovine serum (FBS), and phosphate buffered saline (PBS). The following compounds were obtained from Sigma-Aldrich (Castle Hill, New South Wales, Australia): HAT media supplement Hybri-Max[TM], capsaicin, collagenase, protease, menthol, and allyl isothiocyanate (AITC). Oxytocin and vasopressin were a kind gift from Professor Paul Alewood (Institute for Molecular Bioscience, The University of Queensland). Calcium 4 No Wash dye was purchased from Molecular Devices (Sunnyvale, CA, USA).

Cell culture

Human neuroblastoma SH-SY5Y cells (The European Collection of Cell Cultures) were grown in Roswell Park Memorial Institute medium with 15% FBS and 2 mM L-glutamine and kept at 37°C/5% CO_2; 0.25% trypsin/EDTA was used to passage the cells every three to five days at a 1:5 dilution ratio or when approximately 90% confluent.

Mouse neuroblastoma/rat embryonic DRG neuron hybrid F-11 cells (The European Collection of Cell Cultures) were grown in Ham's F12 media with 10% FBS, 100 mM hypoxanthine, 0.4 mM aminopterin, and 16 mM thymidine (HAT media supplement Hybri-Max[TM]) and kept at 37°C/5% CO_2; 0.25% trypsin/EDTA was used to passage the cells every two to three

days at a 1:5 dilution ratio or when approximately 80% confluent.

Mouse neuroblastoma/rat DRG neuron hybrid ND7/23 cells (The European Collection of Cell Cultures) were grown in DMEM with 10% FBS, 2 mM L-glutamine, pyridoxine, and 110 mg/ml sodium pyruvate and kept at 37°C/5% CO_2; 0.25% trypsin/EDTA was used to passage the cells every three to five days at a 1:5 dilution ratio or when approximately 90% confluent.

Sample extraction and preparation

Mice were euthanised with carbon dioxide followed by cervical dislocation. The spine was immediately removed, the dorsal side of the vertebra bones removed, and the tissue immersed in ice-cold DMEM. The spinal cord was removed, and thoracic and lumbar DRGs (T6-L6 inclusive) were dissected with forceps and placed in DMEM, followed by trimming of excess myelin. Dissected DRGs were then placed into fresh DMEM with 1 mg/mL collagenase and 0.5 mg/mL protease, and incubated at 37°C/5% CO_2 for 45 min to allow for dissociation. The dissociated cells were centrifuged at 20,000 r/min for 3 min and excess DMEM removed. The cell pellet was then washed in PBS, centrifuged briefly, and excess PBS removed. Whole DRG samples from two mice were pooled together for RNA extraction.

All cell lines were allowed to reach ∼90% confluence in a T75 flask in culture before harvesting. Cells were harvested by washing with PBS, followed by trypsinisation with 0.25% trypsin/EDTA. The appropriate cell culture media were added into the flask and the cell suspension was centrifuged at 14,000 r/min for 5 min to form a pellet. Excess media was removed and the cell pellet processed for RNA extraction.

RNA-seq, bioinformatics analysis, and data analysis

Cells were brought up from frozen stocks and allowed to recover for at least three to five passages. RNA was extracted from SH-SY5Y cells at passage 29, from F-11 cells at passage 9, and from ND7/23 cells at passage 28 using the RNeasy Mini Kit (Qiagen, Melbourne, Australia) according to the manufacturer's instructions, including on-column DNase digestion. The RNA Integrity Number (RIN) was above 8.5 for all samples. Library construction and bioinformatics analysis were conducted by the Australian Genome Research Facility. RNA-Seq was conducted on an Illumina Hiseq-2000 machine as a 100-nucleotide single-end run, and primary.fastq data was generated with the CASAVA 1.8.2 pipeline (Illumina). Reads were screened for the presence of any adaptor or overrepresented sequences, ambiguous characters were clipped where required, and sequence bias was corrected. Alignment was performed with Tophat with default analysis parameters in single-end mode. The number of mismatches were restricted to no more than two bases. Reads from SH-SY5Y cells were mapped against the human genome (hg19), DRG reads were mapped against the mouse genome (mm9), and F-11 and ND7/23 reads were mapped against both the mouse genome (mm9) and rat genome (rn5). Transcripts assembly was performed by Cufflinks with the reference annotation-based assembly option[14] using the UCSC annotation, and multi-reads correction was used. Gene counts were then compiled using the HTSeq software.[15] Heatmaps were generated using R with the gplots, pheatmap, and RColorBrewer libraries.

Accession number and gene ontology analysis

Raw bioinformatics data in the form of .fastq files and count tables generated with HTSeq are both available at the Gene Expression Omnibus database under the accession number GSE75811. Gene ontology (GO) analysis was conducted with the PANTHER database[16] with the Gene List Analysis tool.[17] Genes with >100 reads in each sample were compiled and submitted to Gene List Analysis and analysed according to Biological Processes (BP) terms. Genes from whole DRGs were assigned according to the *Mus musculus* genome, the SH-SY5Y sample was assigned to the *Homo sapiens* genome and F-11 and ND7/23 samples were assigned to both *Mus musculus* and *Rattus norvegicus* genomes each.

Transfection

HEK293 (American Tissue Culture Collection, Manassas, VA, USA) were routinely maintained in DMEM containing 10% FBS, 2 mM L-glutamine, pyridoxine, and 110 mg/ml sodium pyruvate. Cells were split every three to six days in a ratio of 1:5 using 0.25% trypsin/EDTA. Cells were plated on T75 tissue culture flasks (Nunc) 24 h prior to transfection, and transfected with plasmid DNA of rTRPV1 (D. Julius, Department of Physiology, University of California, Berkeley, CA, USA), mTRPA1 (A. Patapoutian, The Scripps Research Institute, La Jolla, CA, USA), rTRPM8 (K. Zimmermann, Department of Anesthesiology, Friedrich-Alexander-University, Erlangen-Nuremberg, Erlangen, Germany), hV1A, or hOTR (OriGene Technologies, Rockville, MD, USA) using Lipofectamine 2000 according to the manufacturer's instructions. Twenty-four hours after transfection, cells were plated on 384-well plates and used for Ca^{2+} experiments 24 h after plating.

Fluorescent Ca^{2+} assays

Cells were prepared as previously reported.[9] Briefly, cells were seeded onto 384-well black-walled imaging plates

(Corning, MA, USA) 48 h prior to calcium imaging experiments and incubated at 37°C/5% CO_2. SH-SY5Y cells were placed onto uncoated plates (Corning, Cat No #3542), while F-11 and ND7/23 cells were placed onto Cell-bind (Corning, Cat no #3683) plates. Cells were seeded to ensure ~90% confluency on the day of the experiment.

Cells were loaded 30 min prior to imaging with Calcium 4 No-Wash dye in physiological salt solution (PSS; NaCl 140 mM, glucose 11.5 mM, KCl 5.9 mM, $MgCl_2$ 1.4 mM, NaH_2PO_4 1.2 mM, $NaHCO_3$ 5 mM, $CaCl_2$ 1.8 mM, HEPES 10 mM), and kept at 37°C/5% CO_2. Ca^{2+} responses were measured using a FLIPR^{TETRA} (Molecular Devices, Sunnyvale, CA, USA) fluorescent plate reader with excitation at 470–495 nM and emission at 515–575 nM. Camera gain and intensity were adjusted for each plate to yield a minimum of 1000–1500 arbitrary fluorescence units baseline fluorescence. Prior to addition of agonists, 10 baseline fluorescence readings were taken, followed by fluorescent readings every 0.5 s for 150 s. Data was analysed using Screenworks 3.2 and FLIPR^{TM} data were plotted using GraphPad Prism^{TM} software (Version 6.00).

Results

All samples had 84% or more reads aligned to the respective reference genomes (Table 1). The whole DRG sample included heterogenous populations of cells including neurons and non-neuronal cells, as exemplified by the presence of the non-neuronal glial cell marker vimentin (*VIM*).[18] All cell samples expressed the neuronal and glial marker N-Cam, the neuronal marker F-3, and the mouse neuronal marker Thy-1, which was particularly abundant in the whole DRG sample. As data normalisation relies upon housekeeping genes expressed in similar levels across all samples, we examined the expression of various housekeeping genes due to the recognised issue of differential expression levels for standard housekeeping genes[19] and found *TUBA1A* to be one of the only candidates expressed at a similar global level (0.02–0.08% of all aligned reads) across all samples in our data. In contrast, other popular housekeeping genes commonly used in data normalisation, such as GAPDH and β-actin, were not expressed with similar intensity across all our samples. For instance, 64 reads aligned to GAPDH in the DRG sample, while 12,475 reads aligned to GAPDH in the SH-SY5Y sample. We thus normalised all reads to the highly expressed α-tubulin gene, with the intensities of gene expression presented as normalised gene ratios.

The two hybrid cell lines examined, F-11 and ND7/23, are known to contain both rat and mouse chromosomes (F-11)[8] and express rat surface markers after fusion with mouse neuroblastoma cells (ND7/23).[7] It was not clear which genes are transcribed from the rat genome and which are from the mouse genome in these cell lines. We therefore chose to align F-11 and ND7/23 reads twice, once against the mouse genome and once against the rat. We found that qualitatively, expression profiles largely mirrored each other between mouse and rat alignments in these two cell lines, varying predominantly in intensity.

Neuronal markers expressed by neuronal cell lines

We initially analysed the cell line expression data against a wide range of known markers of specific neuronal types (Figure 1(a)). Some of these include the peptidergic nociceptor marker TrkA (*NTRK1*), the mechanosensor marker *PIEZO2/FAM38B*, the myelinated neuronal marker *CNTNAP2* (contactin associated protein-like 2), and voltage-gated calcium channel (Ca_V) subtype 3.2 that was recently identified to be uniquely expressed on unmyelinated low-threshold mechanoreceptors (C-LTMR)[20] (*CACNA1H*). Out of the 43 neuronal markers investigated, transcripts of nine were found in all cell lines. These nine genes included the nociceptor markers voltage-gated sodium channel (Na_V) subtype 1.9 (*SCN11A*) and acid-sensing ion channel 1 (*ASIC1*); *TLX3*, a transcription factor that regulates the expression of several sensory channels and receptors implicated

Table 1. Read alignments for all RNA samples.

	Mouse DRGs (mm9)	SH-SY5Y (hg19)	F-11 (mm9)	F-11 (rn5)	ND7/23 (mm9)	ND7/23 (rn5)
Total reads	35723774	31364133	29496604	13580565	30759267	12005128
Aligned reads	32480739 (90.92%)	27118145 (86.46%)	26346262 (89.32%)	11513489 (84.78%)	27667233 (89.95%)	10337475 (86.11%)
Non-matching reads	2217836 (6.83%)	2407972 (7.68%)	2346986 (7.96%)	1987513 (14.63%)	2225020 (7.23%)	1612465 (13.43%)
Multiple matching reads	1025199 (3.15%)	1838016 (5.86%)	803356 (2.72%)	47147 (0.59%)	867014 (2.82%)	42507 (0.46%)

DRG: dorsal root ganglion.
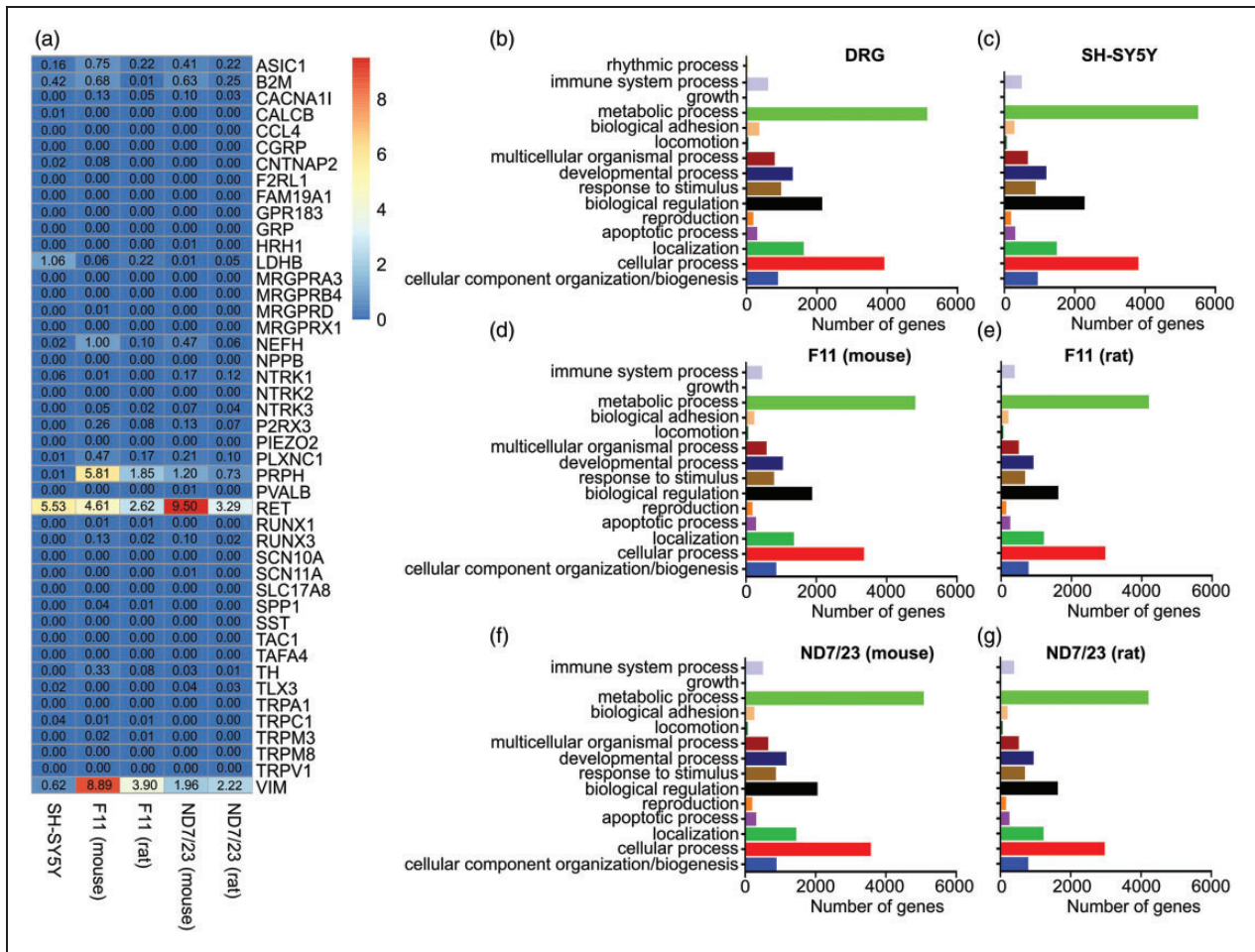
Figure 1. Neuronal markers and gene ontology analysis on RNA samples. The SH-SY5Y, F-11, and ND7/23 cell lines do not fit into existing categories of peripheral neurons, yet gene ontology analysis demonstrates that the cell lines transcriptomes retain similar ratios of enriched biological processes compared to whole DRGs. (a) Expression of markers commonly used to identify specific peripheral neuron sub-populations, microglia, and non-neuronal cells by the SH-SY5Y, F-11, and ND7/23 cell lines. (b) Gene ontology analysis of whole DRGs. (c) Gene ontology analysis of SH-SY5Y cells. (d) Gene ontology analysis of F-11 cells (aligned to the mouse genome). (e) Gene ontology analysis of F-11 cells (aligned to the rat genome). (f) Gene ontology analysis of ND7/23 cells (aligned to the mouse genome). (g) Gene ontology analysis of ND7/23 cells (aligned to the rat genome).

in sensing pain, itch, and temperature[21]; *PLXNC1*, a marker for unmyelinated nonpeptidergic nociceptors and thermosensors; *RET*, a marker for myelinated and unmyelinated neurons;[22] the C-LTMR marker tyrosine hydroxylase (*TH*);[23] *RUNX3*, a transcription factor that regulates the development of proprioceptive DRG neurons[24]; the unmyelinated C-fibre marker peripherin (*PRPH*); and *LDHB*, a marker of myelinated neurons[22] (Figure 1(a)). However, the co-expression of some of these markers in individual cell lines was surprising given their expression profiles do not overlap significantly in subtypes of DRG neurons. Specifically, some markers are known to be selectively expressed in unmyelinated C-fibre neurons (such as *PRPH* and *TH*), while others are indicative of myelinated A-fibres (such as

LDHB) and would thus not be expected to be present in a single sensory neuron type. Many sensory neuron genes were also absent across all cell line samples, including nociceptive markers such as *TRPV1*,[25] *TRPA1*,[26] calcitonin gene-related peptide (*CGRP*),[27] and Na$_V$1.8 (*SCN10A*); mechanoreceptor markers such as *PIEZO2*[28] and *VGLUT3/SLC17A8*[29]; and markers for neurons responsible for itch such as PAR2 (*F2RL1*).[30] This suggests that while the cell lines are known to express receptors found on DRG neurons, they do not mimic the entire repertoire of proteins expressed by functional in vivo DRG neuron classes.

In SH-SY5Y cells, the most enriched marker was *RET*, the glial cell line-derived neurotrophic factor (GDNF) receptor tyrosine kinase, consistent with

previous reports that these cells respond to GDNF with increased neurite outgrowth.[31,32] SH-SY5Y cells expressed markers of A-fibres, including *LDHB*, *CNTNAP2*, and neurofilament heavy polypeptide (*NEFH*). However, TrkA (*NTRK1*), a C-fibre marker, was also expressed; while the A-fibre marker TrkC (*NTRK3*) was completely absent. SH-SY5Y also lacked the nociceptor markers *TRPV1*, MAS-related GPR member D (*MRGPRD*), the peptidergic neuron markers *CGRP*, substance P (*TAC1*), the itch receptor marker somatostatin, the mechanoreceptor marker *TAFA4/FAM19A4*, and the proprioceptor marker parvalbumin (*PVALB*). Overall, SH-SY5Y cells expressed a range of genes associated with different subtypes of sensory neurons and could not be classified according to known DRG neuron subclasses, including those defined by Usoskin et al.,[22] Li et al.,[33] or simpler categorisation based on expression of established markers relating to functional aspects, such as CGRP, IB4, and NF200. Although further classification of sensory neurons was recently reported by Li et al.,[33] DRG classification criteria based on transcriptional markers remain relatively broad and as yet do not unambiguously encompass the possibly 17 or more different fibre types that have been proposed based on responsiveness to mechanical and thermal stimuli as well as conduction velocity and rate of adaptation.[34] Thus, while these cells express genes – as well as their respective protein products[9,10] – known to be involved in key sensory neuron functions, they should not be regarded as a model for DRG neurons.

F-11 and ND7/23 cells were both created from a fusion of mouse neuroblastoma cells and rat embryonic or neonatal DRG neurons, respectively.[7,8] Accordingly, the expression profile of neuronal markers was similar in both cell lines, and included a number of markers of A-fibre mechanosensors and proprioceptors, including *LDHB*, *NEFH*, and *TrkC* (Figure 1(a)). As with SH-SY5Y cells, markers for C-fibres were also present in both cell lines, including *P2RX3*, a purinergic ion channel expressed in C-fibre non-peptidergic neurons; plexin C1 (*PLXNC1*); *TH*; *PRPH*; *RET*; and $Ca_V3.3$ (*CACNA1I*). ND7/23 cells expressed comparatively higher levels of *TLX3*, *SCN11A*, TrkC, and TrkA than F-11 cells, while *ASIC1*, *PLXNC1*, *TH*, *PRPH*, *NEFH*, *CNTNAP2*, *LDHB*, *CACNA1H*, and *CACNA1I* had reduced expression in ND7/23 cells compared with F-11 cells. TrkB was expressed at very low levels in both cell lines. The C-fibre marker TrkA was enriched approximately 20-fold in ND7/23 cells compared with F-11 cells, while *TH* was elevated approximately 10-fold in F-11 cells compared to ND7/23 cells. This established that, similar to SH-SY5Y cells, both F-11 and ND7/23 cells expressed a range of cellular markers that are usually found in distinct sensory neuron subtypes and a specific neuronal origin can thus not be definitely assigned.

All samples showed a similar distribution of genes expressed according to BP terms following global GO analysis. The BP term with the most genes associated was 'metabolic process' across all samples, followed by the terms 'cellular process' and 'biological regulation'. Fourteen different BP terms were found to be present in all samples, with whole DRGs being the only sample that contained one extra term, that of 'rhythmic process' (Figure 1(b) to (g)). F-11 and ND7/23 samples exhibited reduced numbers of genes associated with each BP term when analysed against the rat genome; however, the distribution of associations across different terms remains very similar across the mouse and rat genomes for both samples.

Ion channel and GPCR expression by neuronal cell lines

We next analysed the expression of ion channels and GPCRs in whole DRGs and F-11, ND7/23, and SH-SY5Y cells. Ion channels have an important role in regulating neuronal excitability and firing rate, making them promising novel therapeutic targets in the treatment of pain. Pharmacological modulators of certain families of ion channels, including voltage-gated calcium channels (Ca_V), voltage-gated potassium channels (K_V), and voltage-gated sodium channels (Na_V), are already used as drugs in the clinic to treat neuropathic pain.[35,36] Similarly, many GPCRs initiate intracellular changes after activation from external chemicals, making this family of receptors ideal pharmacological targets. A number of GPCRs are already effective and established analgesic targets, such as the opioid receptors, while others have recognised roles in inflammation and nociception, such as bradykinin and protease-activated receptors.[37–39] We assessed expression of ion channels and GPCRs with putative therapeutic importance based on classification obtained from IUPHAR (http://www.guidetopharmacology.org).

There were 261 ion channel genes detected in whole DRGs ($\geqslant$1 read aligned to the gene), 217 in SH-SY5Y cells, 223 in F-11 (mouse), 201 in F-11 (rat), 214 in ND7/23 (mouse), and 189 genes in ND7/23 (rat). Twenty-one families of ion channels were expressed by all samples, including several considered as therapeutic targets for pain such as ASIC receptors, $GABA_A$ receptors, and voltage-gated sodium, potassium, and calcium channels (Figure 2(a)). Whole DRGs had the highest number of ion channel transcripts among the samples, with 494,237 reads aligned to ion channel genes. The level of ion channel expression was also at least three times higher in whole DRGs (1.42% of total aligned reads) than in the cell lines examined; 0.53% of total aligned reads in SH-SY5Y cells consisted of ion channel reads, while ion channel reads made up 0.43% of total aligned reads in
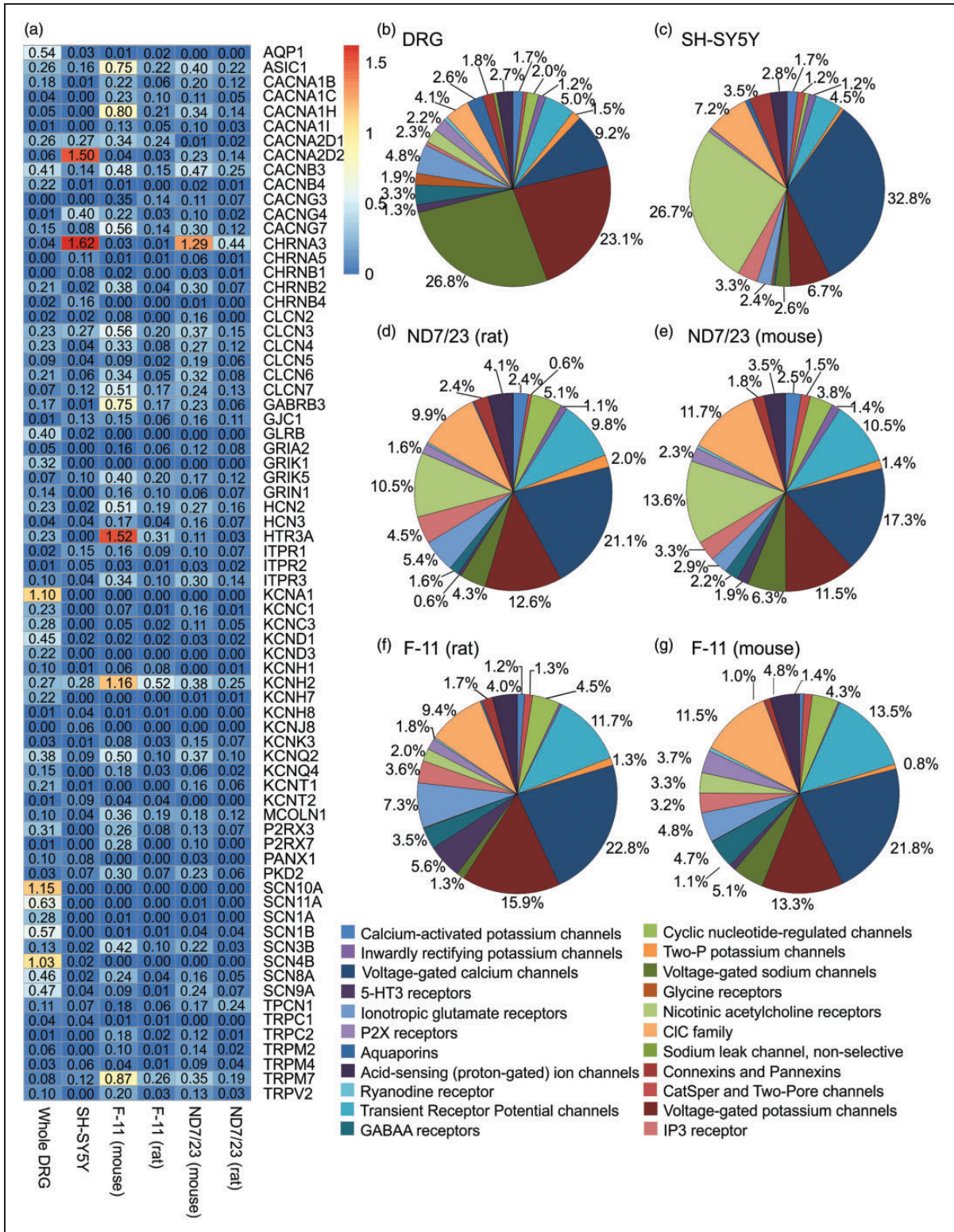
Figure 2. Whole DRGs and cell lines have unique expression patterns of ion channels families. Sections of the pie chart without an annotated percentage constituted ≤ 0.5% of total ion channel expression in the sample. (a) Compilation of the ion channel genes with the highest expression levels for each sample. (b) Distribution of ion channel expression in whole DRGs. (c) Distribution of ion channel expression in SH-SY5Y cells. (d) Distribution of ion channel expression in ND7/23 cells (aligned to the rat genome). (e) Distribution of ion channel expression in ND7/23 cells (aligned to the mouse genome). (f) Distribution of ion channel expression in F-11 cells (aligned to the rat genome). (g) Distribution of ion channel expression in F-11 cells (aligned to the mouse genome).

F-11 (mouse), 0.48% of total aligned reads in F-11 (rat), 0.42% of total aligned reads in ND7/23 (mouse), and 0.45% of total aligned reads in ND7/23 (rat). A total of 58 ion channels were found to be uniquely expressed in whole DRGs, while eight uniquely expressed ion channel genes were found in SH-SY5Y, three in F-11, and four in ND7/23 (Table 2).

The most striking difference in the distribution of ion channel transcripts between DRGs and cell lines lies in the percentage of voltage-gated sodium, potassium, and calcium channels. Together, Na_V, K_V, and Ca_V consisted of 59% of all reads aligned to ion channels in whole DRG, a trend that was reflected in the three cell lines. Na_V, K_V, and Ca_V constituted 43% of all ion channel transcripts in SH-SY5Y cells, 40% in F-11 cells (mouse and rat), 35% in ND7/23 cells (mouse), and 38% in ND7/23 cells (rat) counts. However, much of the Ca_V expression in the cell lines was contributed by Ca_V auxiliary units rather than the channel-forming Ca_V α units, and this was especially true for SH-SY5Y cells. SH-SY5Y cells also abundantly expressed cholinergic nicotinic receptors, amounting to 27% of all ion channel transcripts. In contrast, cholinergic nicotinic receptors consisted of 15% or less ion channel transcripts in all other samples (whole DRG 2%, F-11 mouse 3%, F-11 rat 2%, ND7/23 mouse 14%, and ND7/23 rat 11%) (Figure 2(b) to (g)).

A compilation of the 30 ion channels with the highest expression in each sample revealed significant differences as well as similarities between the cell lines and compared with whole DRGs (Figure 2(a)). The ion channels with the highest expression in whole DRGs were $Na_V1.8$ (*SCN10A*), $K_V1.1$ (*KCNA1*), and Na_V β4 subunit (*SCN4B*). Other ion channels highly expressed in whole DRGs, but expressed at very low levels in the cell lines, included $Na_V1.9$, aquaporin 1, the Na_V β1 subunit, $K_V4.1$ (*KCND1*), and glycine receptor β unit (*GLRB*). In addition, transcripts for $Na_V1.1$ (*SCN1A*), ionotropic glutamate receptor 1 (*GRIK1*), and $K_V4.3$ (*KCND3*) were found at lower levels in DRGs but were virtually absent in the three cell lines. Transcripts for *SCN8A* ($Na_V1.6$) and *SCN9A* ($Na_V1.7$), channels responsible for signal transduction and known to have important roles in pain, were present in all cell lines as well as being highly expressed in whole DRGs. F-11 and ND7/23 cells in particularly expressed $Na_V1.6$ and $Na_V1.7$ at higher levels than SH-SY5Y cells, with F-11 cells expressing more $Na_V1.6$ than ND7/23, and ND7/23 cells expressing more $Na_V1.7$ than F-11 cells.

The nicotinic cholinergic receptor α3 (*CHRNA3*) was the ion channel with the highest expression in SH-SY5Y and ND7/23 cells, but few transcripts were found in whole DRGs and F-11 cells. The second-most enriched ion channel in SH-SY5Y cells, the Ca_Vα2δ subunit 2 (*CACNA2D2*), also had very little expression in the

Table 2. Ion channels and GPCRs uniquely expressed in whole DRGs and cell lines.

	Whole DRGs	SH-SY5Y	F-11	ND7/23
Uniquely expressed ion channels	ANO1	AQP10	CATSPER2	KCNK6
	AQP4	AQP3	GJB3	KCNN3
	ASIC2	CHRND	MCOLN3	SCNN1A
	CACNA1D	GABRQ		TRPM5
	CACNA1E	GJC2		
	CACNA2D3	KCNJ8		
	CHRNA6	KCNQ1		
	CHRNB3	SCNN1D		
	GABRA1			
	GABRA2			
	GABRA3			
	GABRA5			
	GABRB2			
	GABRG1			
	GABRG2			
	GABRG3			
	GJB1			
	GJC3			
	GJD2			
	GRIA1			
	GRID2			
	GRIK1			
	GRIK4			
	GRIN3A			
	HCN1			
	HVCN1			
	KCNA1			
	KCNA2			
	KCNB2			
	KCNC2			
	KCND3			
	KCNG2			
	KCNG4			
	KCNH5			
	KCNJ16			
	KCNJ3			
	KCNJ9			
	KCNK10			
	KCNK13			
	KCNK18			
	KCNK4			
	KCNQ3			
	KCNS1			
	KCNU1			
	KCNV1			
	NALCN			
	P2RX5			
	RYR3			
	SCN10A			
	SCN1A			

Table 2. Continued

	Whole DRGs	SH-SY5Y	F-11	ND7/23
	SCN4A			
	SCN2B			
	TRPA1			
	TRPC4			
	TRPC6			
	TRPM3			
	TRPM8			
	TRPV1			
Uniquely expressed GPCRs	ADRA1D	APLNR	GPBAR1	AGTR2
	ADRA2A	GPR63		DRD2
	ADRB2	GPR98		DRD4
	AGTR1B	HTR2B		GIPR
	CCKAR	LTB4R1		GPR20
	CHRM2	NPFFR2		GPR4
	CYSLTR2	PTGER2		HRH3
	DARC	PTH2R		SSTR5
	ELTD1			TAS1R2
	GABBR2			VIPR2
	GALR1			
	GPR126			
	GPR139			
	GPR149			
	GPR179			
	GPR26			
	GPR35			
	GPR37L1			
	GPR61			
	GPR75			
	GPR83			
	GRM4			
	GRM8			
	HCRTR1			
	HCRTR2			
	HRH1			
	HTR1A			
	HTR1B			
	HTR1D			
	HTR1F			
	HTR2A			
	HTR4			
	HTR5A			
	HTR7			
	LPAR5			
	MCHR1			
	MRGPRD			
	MRGPRX1			
	NPY1R			
	OPRK1			
	OXTR			
	P2RY1			
	P2RY12			

(continued)

Table 2. Continued

	Whole DRGs	SH-SY5Y	F-11	ND7/23
	PTGDR			
	PTGER3			
	S1PR1			

GPCR: G-protein coupled receptor; DRG: dorsal root ganglion. A gene is considered to be uniquely expressed if >100 reads are detected only in one sample.

other samples. Other ion channels highly expressed in SH-SY5Y cells included Ca$_V$ auxiliary units such as *CACNG4* and *CACNA2D1*, and voltage-gated chloride channels such as *CLCN3* (Figure 2(a)).

While the overall gene expression profiles of F-11 and ND7/23 cells were similar, there was notable disparity in ion channel expression. F-11 cells expressed a large amount of transcripts for K$_V$11.1 (*KCNH2*, otherwise known as Human ether-a-go-go-related gene (*hERG*)) and 5-HT receptor 3 a (*HTR3A*), genes that were expressed at much lower level in ND7/23 cells (Figure 2(a)). In contrast, *CHRNA3* was the most highly expressed ion channel transcript in ND7/23 cells, but was only expressed at low levels in F-11 cells. Apart from these exceptions, many ion channel genes where expressed at similar levels in F-11 and ND7/23 cells. Several of these, including ion channels with recognised roles in nociception such as *ASIC1*, Ca$_V$3.2 (*CACNA1H*), and K$_V$7.2 (*KCNQ2*) were highly expressed in F-11 and ND7/23 cells as well as in whole DRGs and SH-SY5Y cells (Figure 2(a)). Similarly, *P2RX3*, Ca$_V$3.3 (*CACNA1I*), *TRPV2*, and Ca$_V$2.2 (*CACNA1B*) were enriched in F-11 and ND7/23 cells to a lesser extent compared with DRGs and SH-SY5Y cells. For all of these ion channels, transcript numbers were higher in F-11 cells compared with ND7/23 cells. In contrast, *TRPM2*, *CLCN2*, *KCNK3*, *CLCN5*, *GRIA2*, *TPCN1*, *KCNC3*, *KCNC1*, and *KCNT1* were expressed at higher levels in ND7/23 cells than F-11 cells.

A total of 300 different GPCR genes from the IUPHAR list were expressed in whole DRGs, 218 genes in SH-SY5Y cells, 215 in F-11 (mouse), 188 in F-11 (rat), 225 in ND7/23 (mouse), and 187 in ND7/23 cells (rat) (Figure 3(a) to (g)). Whole DRGs contained the most GPCR transcripts, with 185,707 reads aligned to GPCR genes accounting for 0.54% of all aligned reads. SH-SY5Y cells had the second-most abundant GPCR expression (0.38% of all aligned reads), followed by ND7/23 mouse (0.35%), ND7/23 rat (0.33%), and F-11 rat and mouse (both 0.26%). Similar to the trend seen for ion channels, whole DRGs had both the highest GPCR expression level and the highest number of uniquely expressed GPCRs, with 46 GPCRs uniquely
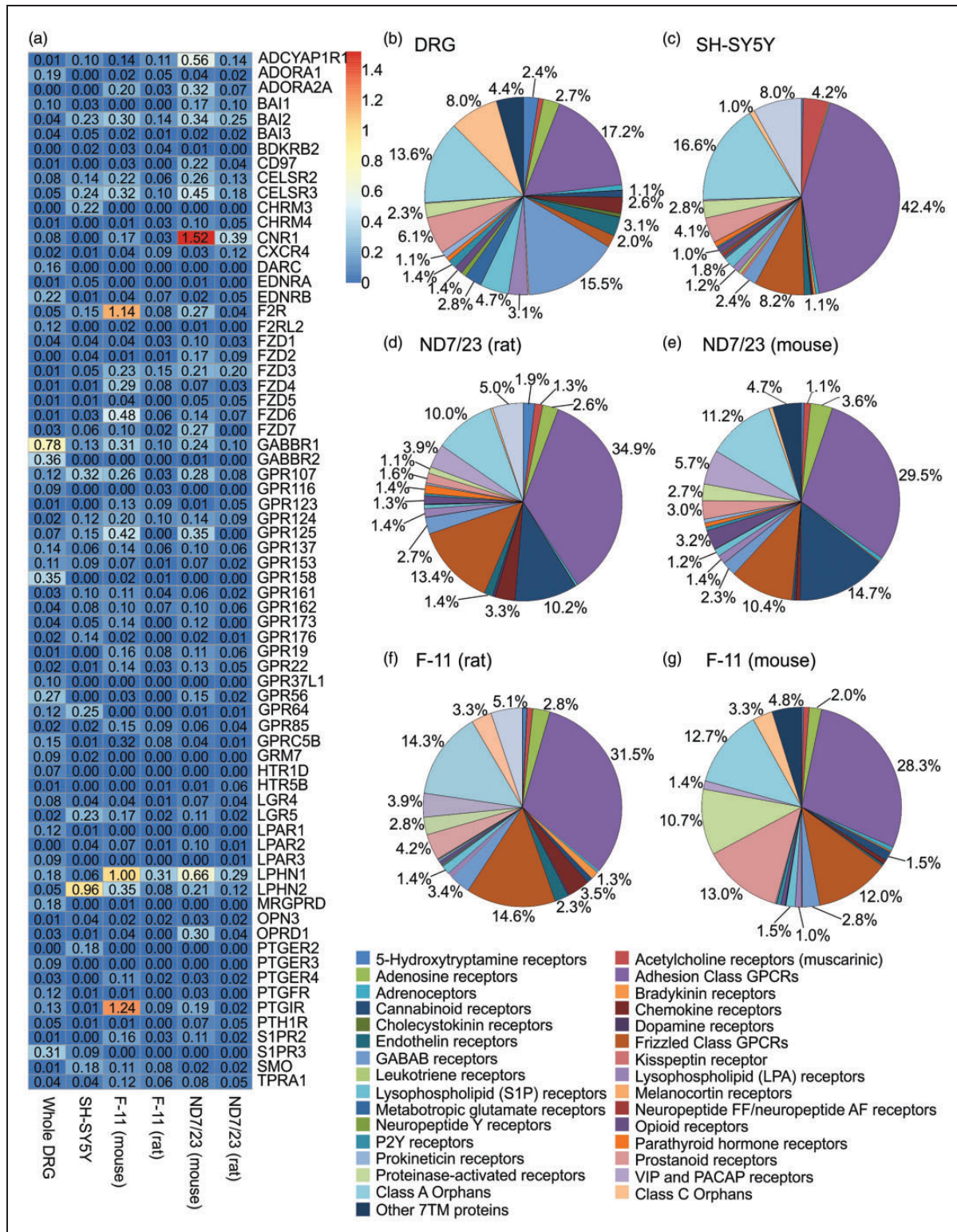
Figure 3. Whole DRGs and cell lines have unique expression patterns of GPCRs. Sections of the pie chart without an annotated percentage constituted ⩽0.5% of total ion channel expression in the sample. (a) Compilation of the GPCR genes with the highest expression levels for each sample. (b) Distribution of GPCR expression in whole DRGs. (c) Distribution of GPCR expression in SH-SY5Y cells. (d) Distribution of GPCR expression in ND7/23 cells (aligned to the rat genome). (e) Distribution of GPCR expression in ND7/23 cells (aligned to the mouse genome). (f) Distribution of GPCR expression in F-11 cells (aligned to the rat genome). (g) Distribution of GPCR expression in F-11 cells (aligned to the mouse genome).

expressed in whole DRGs. SH-SY5Y cells expressed 8 unique GPCRs, F-11 cells expressed 1, and ND7/23 cells expressed 10 (Table 2).

A total of 45 families of GPCRs were expressed by all four samples. Among these, the adhesion class GPCR family had the highest expression levels in all samples, constituting 42% of all GPCR transcripts from SH-SY5Y cells, 35% in ND7/23 cells (rat), 32% in F-11 cells (rat), 28.3% in ND7/23 (mouse), 27.5% in F-11 (mouse), and 17% in whole DRGs. The GPCR family with the second highest expression in whole DRGs were the GABA$_B$ receptors GABBR1 and GABBR2 (16% of all GPCR reads), a trend that was not observed in the cell lines where GABA$_B$ receptors only consisted of 3% of GPCR reads in F-11 and ND7/23 (rat) and 2% in ND7/23 (mouse) and SH-SY5Y cells. However, expression of approximately equivalent transcript numbers for both the R1 and R2 subunit of the GABA$_B$ receptor was only observed in DRG neurons, suggesting that functional GABA$_B$ receptors do not form in the neuronal cell lines (Figure 3(b)).

Other GPCRs with high expression in whole DRGs include sphingosine-1-phosphate receptor 3 and the orphan GPCRs GPR158 and GPR56. These genes, together with the prostaglandin F receptor (PTGFR), par3 (F2RL2), 5-HT receptor 1D (HTR1D), prostaglandin E receptor 3 (PTGER3), and adenosine A1 receptor (ADORA1), were expressed at very low levels in neuronal cell lines. Two exceptions in this group include the orphan GPCRs with unknown function, GPR137, and GPR153, which were expressed in all samples (Figure 3(a)).

The GPCR with the highest level of expression in SH-SY5Y cells was latrophilin 2 (LPHN2). Latrophilin 2 is an adhesion GPCR that plays a role in exocytosis and is closed related to latrophilin 1 (LPHN1), the receptor for latrotoxin, the active peptide in black widow spider venom.[40] Interestingly, latrophilin 1 was the GPCR with the highest expression in F-11 cells and the second highest expressed in ND7/23 cells, and was also present in whole DRGs. Many genes enriched in SH-SY5Y cells, such as smoothened and par1 (F2R), were also expressed in other samples. However, a small group of genes, including the muscarinic acetylcholine receptor M3 (CHRM3) and prostaglandin E2 receptor (PTGER2), were enriched in SH-SY5Y cells but largely absent in other samples. Overall, GPCR expression patterns were similar for all neuronal cell lines, but distinct from that of whole DRGs (Figure 3(a)).

In F-11 cells, the prostaglandin I2 receptor (PTGIR), par1 (F2R), and LPHN1 were the most highly expressed GPCRs. In ND7/23 cells, the GPCRs with the highest expression were the cannabinoid receptor 1, LPHN1, and pituitary adenylate cyclase-activating polypeptide type I receptor. The majority of GPCR genes were

expressed at similar levels in F-11 and ND7/23 cells. GPCRs enriched in F-11 and ND7/23 tended to be expressed at very low levels in whole DRGs, whereas a group of GPCRs highly expressed in DRGs, including CELSR3 and BAI2, were enriched in SH-SY5Y cells. Of note, GPR123 and PTGER4 were enriched exclusively in F-11 cells, and CD97 and FZD2 were enriched only in ND7/23 cells. When aligned to the mouse genomes, the top 30 GPCRs expressed for F-11 and ND7/23 cells resembled each other very closely. Interestingly, F-11 cells expressed mouse but not rat transcripts of PTGIR, while the same was the case for ADCYAP1R in ND7/23 cells (Figure 3(a)).

Interestingly, we noted expression of both arginine vasopressin receptor 1A (AVPR1A) and oxytocin receptors (OXTR) in DRGs, consistent with an emerging functional role of these GPCRs in pain, where AVPRA1 has been linked to strain-dependent pain sensitivity to formalin and capsaicin[41] and oxytocin activation ameliorates visceral pain in particular.[42] Consistent with a specific role of these GPCRs in pain, both vasopressin receptor 1B and vasopressin receptor 2 were expressed at very low level or absent in DRGs. In contrast, all three cell lines expressed OXTRs, but vasopressin receptor 1A and 1B were absent. We thus sought to verify this gene expression profile using functional Ca^{2+} imaging. The OXTR was expressed in SH-SY5Y cells, absent in F-11 cells, and only aligned to three reads in ND7/23 cells. Accordingly, only SH-SY5Y responded to oxytocin at concentrations that elicit Ca^{2+} responses in HEK293 cells transfected with the OXTR, confirming the presence of functional OXTRs in SH-SY5Y cells and its absence in F-11 and ND7/23 cells (Figure 4(a) and (b)). Moreover, consistent with our transcriptomic results, vasopressin did not elicit an increase in intracellular Ca^{2+} in any of the cell lines tested, albeit robust Ca^{2+} responses were elicited in HEK293 cells transiently transfected with AVPR1A (Figure 4(c) and (d)).

The gene expression profiles observed in this study are supported by several studies assessing expression of isolated ion channels and GPCRs in sensory neurons, SH-SY5Y neuroblastoma, as well as F-11 and ND7/23 cells. Specifically, the expression profile of Ca$_V$ transcripts in SH-SY5Y cells was entirely consistent with that previously reported,[11] with Ca$_V$2.1, Ca$_V$2.3, Ca$_V$3.2, and Ca$_V$1.1 being completely absent in SH-SY5Y cells. Ca$_V$3.1 had the largest number of reads, followed by Ca$_V$2.2 and Ca$_V$1.3. SH-SY5Y cells also expressed several Ca$_V$ auxilliary units at high level, a trend that was also observed in F-11 and ND7/23 cell lines. In contrast, the order of expression of Ca$_V$ alpha units in DRGs was observed as Ca$_V$2.2 > Ca$_V$2.1 > Ca$_V$3.2 > Ca$_V$1.2 > Ca$_V$3.3 > Ca$_V$1.3 > Ca$_V$2.3 > Ca$_V$3.1 > Ca$_V$1.1 > Ca$_V$1.4, with all alpha isoforms being present (supplementary data). This was mirrored by the F-11 and the ND7/23
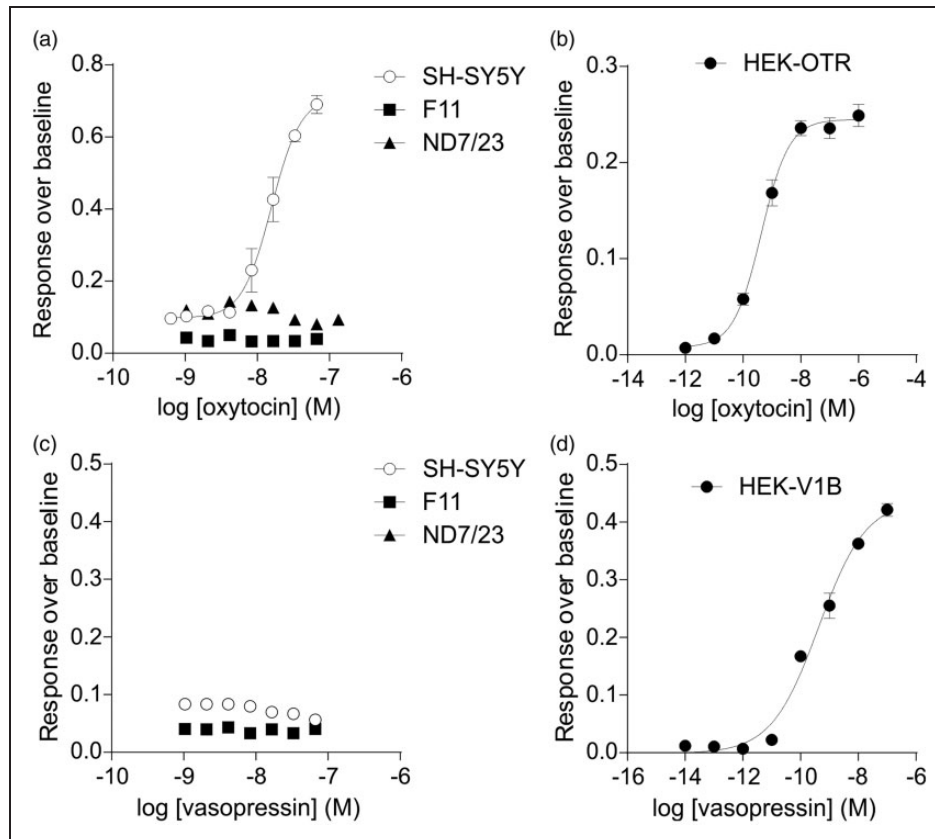
Figure 4. Calcium response to oxytocin and vasopressin addition in DRG neurons and cell lines. Functional oxytocin receptors are expressed in SH-SY5Y cells, but not in F-11 or ND7/23 cells. Functional vasopressin receptors are absent from all three cell lines. (a) Calcium influx responses of SH-SY5Y, F-11, and ND7/23 cell lines upon exposure to oxytocin. (b) Calcium response of HEK293 cells transfected with oxytocin receptor (OXTR) upon exposure to oxytocin. (c) Calcium influx responses of SH-SY5Y, F-11, and ND7/23 cell lines upon exposure to vasopressin. (d) Calcium response of HEK293 cells transfected with the vasopressin V1B receptor (AVPR1B) upon exposure to vasopressin.

cells, both of which expressed all Ca_V isoforms with a similar pattern. F-11 and ND7/23 expressed most $Ca_V 3.2$ out of all Ca_V alpha subunits, closely followed by $Ca_V 2.2$, $Ca_V 1.2$, and $Ca_V 3.3$.

Similarly, expression of *KCNQ2* and *KCNQ3*, the genes encoding $K_V 7.2$ and $K_V 7.3$, the K^+ channel isoforms which underlie the M-current, were consistent with previous results reporting presence of this channel in DRGs,[43] F-11 cells,[44] and SH-SY5Y cells;[45] although curiously, *KCNQ3* was absent in ND7/23 cells. Interestingly, $K_V 1.1$, a key K_V channel regulating excitability in DRG neurons, was found to be virtually absent in all cell lines, where the $K_V 11$ subtype family was expressed most abundantly (55.06% of all K_V transcripts in SH-SY5Y, 58.56% in F-11, and 38.30% in ND7/23), and $K_V 1$ family expression was at least 30-fold lower in all cell line samples compared to whole DRGs. $K_V 11.1$ (*KCNH2*), commonly known as the *hERG*, was the most abundant K_V subtype channel in all three cell line samples. These findings are consistent with previous studies

reporting absence of $K_V 1.1$, and endogenous expression of *hERG*, in these cell lines.[46–48]

The expression profile of TRP channel transcripts was similar across all cell lines. *TRPA1* and *TRPV1*, the TRP channels receptive to the noxious stimuli mustard oil and capsaicin, respectively, were largely missing from the three cell lines. Very small amounts of *TRPV1* were present in the three cell lines and TRPA1 was completely absent. TRPM8, the menthol and cold receptor, was also expressed at very low levels in all cell lines as previously reported. The recently identified cold-sensitive channel *TRPC5*[49] was revealed to be present in whole DRGs and in ND7/23 cells, with very low expression in SH-SY5Y and F-11 cells. *TRPM3*, another novel channel suggested to be a potential nociceptor and thermoceptor,[50] was present in whole DRGs, F-11 cells, and ND7/23 cells, with very low expression levels in SH-SY5Y cells (supplementary data).

These findings were confirmed with fluorescent intracellular calcium measurements after the application of
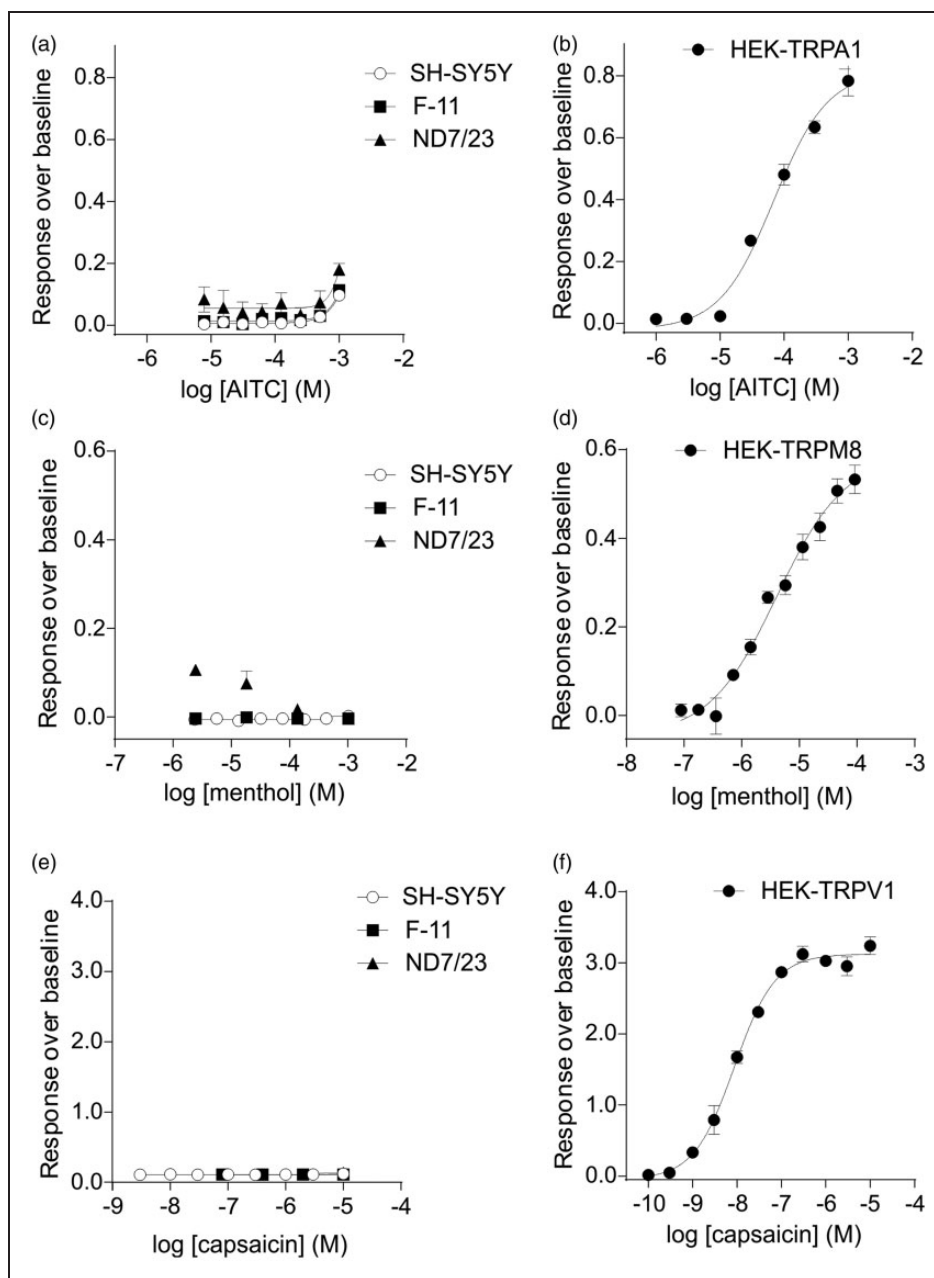
Figure 5. Calcium responses to TRP activators for cell lines and transfected HEK293 cells. Calcium responses to the application of selective TRP activators for cell lines and HEK293 cells transiently expressing TRPA1, TRPM8, or TRPV1. None of the cell lines responded to AITC, menthol, or capsaicin, confirming the absence of TRPA1, TRPM8, and TRPV1 expression in the three cell lines examined. (a) Calcium responses of the cell lines to AITC. (b) Calcium responses of HEK293 cells transiently expressing rat TRPA1 channels to AITC. (c) Calcium responses of the cell lines to menthol. (d) Calcium responses of HEK293 cells transiently expressing rat TRPM8 channels to menthol. (e) Calcium responses of the cell lines to capsaicin. (f) Calcium responses of HEK293 cells transiently expressing rat TRPV1 channels to capsaicin.

selective TRP channel agonists (Figure 5). The *TRPA1* activator, AITC, did not elicit a response from any of the cell lines at concentrations despite activating transfected HEK293 cells transiently expressing rat *TRPA1* (Figure 5(a) and (b)). The application of the *TRPM8* agonist menthol also elicited minimal responses from

any of the three cell lines, while robust Ca^{2+} responses were observed in transfected HEK293 cells (Figure 5(c) and (D)). Similarly, capsaicin, known to activate rat, mouse, and human *TRPV1*,[51–53] elicited no responses in the cell lines, but robustly activated *TRPV1*-transfected HEK293 cells (Figure 5(e) and (F)). The relatively

lack of expression of these key thermosensitive TRP channels suggests that none of the three cell line examined should be used as model nociceptive or thermosensitive neurons.

Discussion

Immortalised neuronal cell lines as models of primary sensory neurons represent a comfortable compromise for the investigation of the neuropharmacological mechanisms underlying pain. These neuroblastoma-derived cell lines often express molecular targets consistent with those found in sensory neurons, bypassing the need for excision and primary culture of tissue while – presumably – retaining endogenous protein expression profiles. Indeed, one advantage of using immortalised neuronal cell lines over heterologously transfected cells is the co-expression of relevant auxillary subunits as well as interacting proteins, and the constellation of channels and receptors that would form the "signallosome" in a native neuron, providing a more holistic insight to nociceptive pharmacology and signalling. However, these properties are often based on assumptions about the gene expression profile of such cell lines, and the lack of comprehensive analyses of receptor expression in these cell lines limits their applicability.

We thus set out to assess the gene expression profile of the model sensory neuron cell lines ND7/23 and F-11 as well as the neuroblastoma cell line SH-SY5Y, which has previously been reported to express genes and ion channels normally restricted to peripheral sensory neurons such as $Na_V1.7$.[10] Accordingly, when compared with the gene expression profile of whole DRG, we found expression of many individual genes known to be expressed in, or play an important role in the function of, sensory neurons. These include *RET*, *TH*, *PRPH*, and *LDHB*. However, we also found many sensory neuron-enriched genes that were absent from the cell lines, such as *TRPV1* and *SCN10A*. Moreover, given that whole DRGs and all three cell lines derive from peripheral neurons, the absence of central nervous system microglial markers such as *CCL4* and *GPR183*[54] in the neuronal cell lines was expected.

Sensory neurons are a heterogeneous group of neurons with distinct functional characteristics and physiological functions. Since cell lines can be considered monoclonal and originate from a single cell colony, the absence of genes enriched in specific subgroups of neurons could be expected – it is plausible that the gene expression profile of ND7/23 and F-11 cells would resemble only one subset of the many different types of sensory neurons. Indeed, both ND7/23 and F-11 cells are often considered a model for small nociceptive neurons that give rise to unmyelinated C-fibres. However, the precise type of sensory neuron that these cell lines may have arisen from, or

that they most closely resemble, is difficult to assess currently, not least because the precise number of individual neuronal subtypes found in DRG are unclear. Based on functional characteristics of the fibres innervating target organs including skin, at least 16 subclasses of purely sensory neurons should exist.[34] In recent years, significant efforts have been made towards identifying the gene expression profile of these individual neuronal classes, as it is becoming increasingly clear that it is the constellation of ion channels, GPCRs, auxiliary subunits, and interacting proteins expressed in a given neuron that defines its functional properties. For example, cold sensitivity in trigeminal neurons is defined by co-expression of $K_V1.1/1.2$ channels with *TRPM8*,[55] while in sensory neurons innervating the skin, a similar functional relationship was observed for *TRPM8* and $K_V7.2/7.3$ channels.[43] There is also existing evidence towards the presence of multiple neuron types within F-11 cell lines,[56] indicating that while neuron-derived cell lines are supposedly clones of the parent cell line, a myriad of neuronal subtypes exists within one population.

Based on a comprehensive study assessing the gene expression profiles of sensory neurons using single-cell RNA sequencing, Usoskin et al.[22] defined four basic sensory neuron subtypes, characterised by expression of *TAC1*, *NTRK1*, and *CALCA* (peptidergic cluster); *MRGPRD* and *P2RX3* (non-peptidergic cluster); *TH* (tyrosine hydroxylase containing cluster); *NEFH* and *PVALB* (neurofilament-containing cluster); as well as 11 subgroups thereof by correlating both old and novel markers to physiological function in peripheral nerves. Li et al.[33] also examined the types of neurons present in DRGs in a separate study, and classified mouse DRG neurons into 10 types and 14 subordinate subtypes based on molecular markers, functional annotations, and transcriptional patterns. The resulting clusters matched the classification by Usoskin et al. to some extent, but also introduced additional transcriptional markers defining subgroups of sensory neurons. Importantly, the gene expression profile of F-11, ND7/23, and SH-SY5Y cells resembled none of these subgroup classifications closely, with all cell lines expressing markers from several different clusters as well as markers of non-neuronal cells including *B2M* and *VIM*.[22] Indeed, F-11 cells expressed high levels of *P2RX3*, *TH*, and *NEFH*, thus simultaneously incorporating markers of non-peptidergic, *TH*-containing, and neurofilament-expressing neurons based on the classification proposed by Usoskin et al.; while ND7/23 cells expressed high levels of the peptidergic neuron marker *NTRK1*, the non-peptidergic marker *P2RX3*, *TH*, and the neurofilament-expressing marker *NEFH*. The corresponding gene modules based on the classifications by Li et al. also belonged to separate clusters, including black (*TH*), turquoise (*P2RX3, NTRK1*), and blue (*NEFH*).[33]

Similar discrepancies were also observed when comparing the gene expression profile of the cell lines to the transcriptome of neurons expressing Na$_V$1.8, which are typically considered nociceptive and expressed high levels of *ANO3*, *TRPA1*, and *CHRNA6*,[57] none of which were present in the immortalised neuronal cell lines examined. However, these discrepancies are perhaps less surprising given none of the cell lines expressed more than one read of Na$_V$1.8 transcripts in the entire sample. Indeed, our results showed that allocation of neuronal cell lines to any single meaningful subtype of sensory neuron is hardly possible, as they expressed a mixture of cellular markers that are typically found in non-overlapping cell populations, including markers for myelinated neurons as well as for unmyelinated neurons. Some examples include the presence of TrkA, TrkB, and TrkC in all cell line samples, suggesting a mixed heritage of the cell lines. Thermosensitive proteins responsible for temperature sensing such as *TRPV1*, *TRPA1*, and *TRPM8* were all virtually absent in the cell lines, making them unlikely to have been derived from thermosensors. The complete lack of *PIEZO2* also indicate that the cell lines are not to be used to investigate stretch-sensitive neurons in their native state.[58] Another subclasses we can rule out are subsets of pruriceptors due to the lack of PAR2 and somatostatin in the cell lines.

Global GO analysis of all samples according to BP terms revealed similar functional distribution of genes, suggesting that these neuronal cell lines maintain broad functional similarities with DRG neurons despite the apparent poor fit into the existing framework of neuron classification. It is possible that despite the lack of expression of certain gene markers, other genes with similar roles are expressed through compensatory mechanisms to maintain functional similarity with *in vivo* peripheral neurons.

While the present study assessed gene expression profiles in undifferentiated ND7/23, F-11, and SH-SY5Y cells, all three cell lines have the capacity and plasticity to develop into mature, terminally differentiated neurons upon exposure to various reagents such as retinoic acid, cAMP derivatives, or forskolin.[45,59] These agents can be used to drive the cells towards various phenotypes away from their native form. This is certainly observed in SH-SY5Y cells, which can express different receptors based on the method used to induce differentiation (for a brief review see Kovalevich and Langford[60]). It is thus possible that differential cells may resemble certain neuronal subtypes more closely, and a transcriptomic analysis on differentiated cells could provide additional insight into processes involved in neuronal maturation.

A drawback of transcriptomic studies lies in difficulties reconciling gene expression with expression of functional proteins. However, we have confirmed the presence of N-methyl-D-aspartate receptors, HCN2 channels, Na$_V$1.7 (*SCN9A*), Ca$_V$2.2, and opioid receptors in all cell lines, consistent with previous findings,[9,10] and we additionally confirmed the observed pattern of expression for selected targets using a pharmacological approach where sufficiently selective agonists were readily available.

Conclusions

To conclude, we present the first comprehensive transcriptomic analysis of the gene expression profile in F-11 and ND7/23 cell lines in comparison with whole mouse DRGs and the human neuroblastoma-derived cell line SH-SY5Y. We found that all cell lines expressed a multitude of receptors and ion channels with relevance to nociceptive signalling. However, although the cell lines investigated express molecular targets found in native DRGs, they are not representative of specific subclasses of peripheral sensory neurons and do not fit into existing peripheral neuron categories. Thus, these findings support the continued use of immortal cell lines with neuronal origins in pain research by defining their gene expression profiles relative to native DRG neurons.

References

1. Fang X, McMullan S, Lawson SN, et al. Electrophysiological differences between nociceptive and non-nociceptive dorsal root ganglion neurones in the rat in vivo. *J Physiol (Camb)* 2005; 565: 927–943. doi:10.1113/jphysiol.2005.086199.
2. Lindsay RM. Nerve growth factors (NGF, BDNF) enhance axonal regeneration but are not required for survival of adult sensory neurons. *J Neurosci* 1988; 8: 2394–2405.

3. Zheng J-H, Walters ET and Song X-J. Dissociation of dorsal root ganglion neurons induces hyperexcitability that is maintained by increased responsiveness to cAMP and cGMP. *J Neurophysiol (Bethesda)* 2007; 97: 15–25. doi:10.1152/jn.00559.2006.

4. Huang Z-J, Li H-C, Cowan AA, et al. Chronic compression or acute dissociation of dorsal root ganglion induces cAMP-dependent neuronal hyperexcitability through activation of PAR2. *Pain* 2012; 153: 1426–1437. doi:10.1016/j.pain.2012.03.025.

5. Genc B, Ulupınar E and Erzurumlu RS. Differential Trk expression in explant and dissociated trigeminal ganglion cell cultures. *J Neurobiol* 2005; 64: 145–156. doi:10.1002/neu.20134.

6. Tsantoulas C, Zhu L, Shaifta Y, et al. Sensory neuron downregulation of the Kv9.1 potassium channel subunit mediates neuropathic pain following nerve injury. *J Neurosci* 2012; 32: 17502–17513. doi:10.1523/JNEUROSCI.3561-12.2012.

7. Wood JN, Bevan SJ, Coote PR, et al. Novel cell lines display properties of nociceptive sensory neurons. *Proc Biol Sci* 1990; 241: 187–194.

8. Platika D, Boulos MH, Baizer L, et al. Neuronal traits of clonal cell lines derived by fusion of dorsal root ganglia neurons with neuroblastoma cells. *Proc Natl Acad Sci USA* 1985; 82: 3499–3503.

9. Vetter I and Lewis RJ. Characterization of endogenous calcium responses in neuronal cell lines. *Biochem Pharmacol* 2010; 79: 908–920. doi:10.1016/j.bcp.2009.10.020.

10. Vetter I, Mozar CA, Durek T, et al. Characterisation of Nav types endogenously expressed in human SH-SY5Y neuroblastoma cells. *Biochem Pharmacol* 2012; 83: 1562–1571. doi:10.1016/j.bcp.2012.02.022.

11. Sousa SR, Vetter I, Ragnarsson L, et al. Expression and pharmacology of endogenous Cav channels in SH-SY5Y human neuroblastoma cells. *PLoS One* 2013; 8: e5923. doi:10.1371/journal.pone.0059293.

12. Biedler JL, Helson L and Spengler BA. Morphology and growth, tumorigenicity, and cytogenetics of human neuroblastoma cells in continuous culture. *Cancer Res* 1973; 33: 2643–2652.

13. Biedler JL, Roffler-Tarlov S, Schachner M, et al. Multiple neurotransmitter synthesis by human neuroblastoma cell lines and clones. *Cancer Res* 1978; 38: 3751–3757.

14. Roberts A, Pimentel H, Trapnell C, et al. Identification of novel transcripts in annotated genomes using RNA-Seq. *Bioinformatics (Oxf)* 2011; 27: 2325–2329. doi:10.1093/bioinformatics/btr355.

15. Anders S, Pyl PT and Huber W. HTSeq—a Python framework to work with high-throughput sequencing data. *Bioinformatics (Oxf)* 2015; 31: 166–169. doi:10.1093/bioinformatics/btu638.

16. Mi H, Muruganujan A and Thomas PD. PANTHER in 2013: modeling the evolution of gene function, and other gene attributes, in the context of phylogenetic trees. *Nucleic Acids Res* 2012; 41: D377–D386. doi:10.1093/nar/gks1118.

17. Mi H, Muruganujan A, Casagrande JT, et al. Large-scale gene function analysis with the PANTHER classification system. *Nat Protoc* 2013; 8: 1551–1566. doi:10.1038/nprot.2013.092.

18. Chiu F-C, Norton WT and Fields KL. The cytoskeleton of primary astrocytes in culture contains actin, glial fibrillary acidic protein, and the fibroblast-type filament protein, vimentin. *J Neurochem* 1981; 37: 147–155.

19. Gubern C, Hurtado O, Rodríguez R, et al. Validation of housekeeping genes for quantitative real-time PCR in in-vivo and in-vitro models of cerebral ischaemia. *BMC Mol Biol* 2009; 10: 57. doi:10.1186/1471-2199-10-57.

20. Reynders A, Mantilleri A, Malapert P, et al. Transcriptional profiling of cutaneous MRGPRD free nerve endings and C-LTMRs. *Cell Reports* 2015; 10: 1007–1019. doi:10.1016/j.celrep.2015.01.022.

21. Lopes C, Liu Z, Xu Y, et al. Tlx3 and Runx1 Act in combination to coordinate the development of a cohort of nociceptors, thermoceptors, and pruriceptors. *J Neurosci* 2012; 32: 9706–9715. doi:10.1523/JNEUROSCI.1109-12.2012.

22. Usoskin D, Furlan A, Islam S, et al. Unbiased classification of sensory neuron types by large-scale single-cell RNA sequencing. *Nat Neurosci* 2015; 18: 145–153. doi:10.1038/nn.3881.

23. Li L, Rutlin M, Abraira VE, et al. The functional organization of cutaneous low-threshold mechanosensory neurons. *Cell* 2011; 147: 1615–1627. doi:10.1016/j.cell.2011.11.027.

24. Inoue K-i, Ozaki S, Shiga T, et al. Runx3 controls the axonal projection of proprioceptive dorsal root ganglion neurons. *Nat Neurosci* 2002; 5: 946–954. doi:10.1038/nn925.

25. Caterina MJ, Leffler A, Malmberg AB, et al. Impaired nociception and pain sensation in mice lacking the capsaicin receptor. *Science* 2000; 288: 306–313.

26. Hoffmann T, Kistner K, Miermeister F, et al. TRPA1 and TRPV1 are differentially involved in heat nociception of mice. *Eur J Pain* 2013; 17: 1472–1482. doi:10.1002/j.1532-2149.2013.00331.x.

27. Ju G, Hokfelt T, Brodin E, et al. Primary sensory neurons of the rat showing calcitonin gene-related peptide immunoreactivity and their relation to substance P-, somatostatin-, galanin-, vasoactive intestinal polypeptide- and cholecystokinin-immunoreactive ganglion cells. *Cell Tissue Res* 1987; 247: 417–431.

28. Woo S-H, Ranade S, Weyer AD, et al. Piezo2 is required for Merkel-cell mechanotransduction. *Nature (Lond)* 2014; 509: 622–628. doi:10.1038/nature13251.

29. Gras C, Herzog E, Bellenchi GC, et al. A third vesicular glutamate transporter expressed by cholinergic and serotoninergic neurons. *J Neurosci* 2002; 22: 5442–5451.

30. Akiyama T, Carstens MI and Carstens E. Excitation of mouse superficial dorsal horn neurons by histamine and/or PAR-2 agonist: potential role in itch. *J Neurophysiol (Bethesda)* 2009; 102: 2176–2183. doi:10.1152/jn.00463.2009.

31. Yamada S, Nomura T, Uebersax L, et al. Retinoic acid induces functional c-Ret tyrosine kinase in human neuroblastoma. *Neuroreport* 2006; 18: 359–363.

32. Park S and Lee J. Proteome profile changes in SH-SY5y neuronal cells after treatment with neurotrophic factors. *J Cell Biochem Suppl* 2011; 112: 3845–3855. doi:10.1002/jcb.23316.

33. Li C-L, Li K-C, Wu D, et al. Somatosensory neuron types identified by high-coverage single-cell RNA-sequencing and functional heterogeneity. *Cell Res* 2016; 26: 83–102. doi:10.1038/cr.2015.149.

34. Zimmermann K, Hein A, Hager U, et al. Phenotyping sensory nerve endings in vitro in the mouse. *Nat Protoc* 2009; 4: 174–196. doi:10.1038/nprot.2008.223.

35. Ocana M, Cendan CM, Cobos EJ, et al. Potassium channels and pain: present realities and future opportunities. *Eur J Pharmacol* 2004; 500: 203–219. doi:10.1016/j.ejphar.2004.07.026.

36. Wallace MS. Ziconotide: a new nonopioid intrathecal analgesic for the treatment of chronic pain. *Expert Rev Neurother* 2006; 6: 1423–1428. doi:10.1586/14737175.6.10.1423.

37. Blaes N and Girolami J-P. Targeting the 'Janus face' of the B2-bradykinin receptor. *Expert Opin Ther Targets* 2013; 17: 1145–1166. doi:10.1517/14728222.2013.827664.

38. Grastilleur S, Mouledous L, Bedel J, et al. Role of kinin B2 receptors in opioid-induced hyperalgesia in inflammatory pain in mice. *Biol Chem Hoppe Seyler* 2013; 394: 361–368. doi:10.1515/hsz-2012-0305.

39. Paterson KJ, Zambreanu L, Bennett DLH, et al. Characterisation and mechanisms of bradykinin-evoked pain in man using iontophoresis. *Pain* 2013; 154: 782–792. doi:10.1016/j.pain.2013.01.003.

40. Bittner MA. α-Latrotoxin and its receptors CIRL (latrophilin) and neurexin 1α mediate effects on secretion through multiple mechanisms. *Biochimie (Paris)* 2000; 82: 447–452.

41. Mogil JS, Sorge RE, LaCroix-Fralish ML, et al. Pain sensitivity and vasopressin analgesia are mediated by a gene-sex-environment interaction. *Nat Neurosci* 2011; 14: 1569–1573. doi:10.1038/nn.2941.

42. ADd Araujo, Mobli M, Castro J, et al. Selenoether oxytocin analogues have analgesic properties in a mouse model of chronic abdominal pain. *Nat Commun* 2014; 5: 3165doi:510.1038/ncomms4165.

43. Vetter I, Hein A, Sattler S, et al. Amplified cold transduction in native nociceptors by M-channel inhibition. *J Neurosci* 2013; 33: 16627–16641. doi:10.1523/JNEUROSCI.1473-13.2013.

44. Jow F, He L, Kramer A, et al. Validation of DRG-Like F11 cells for evaluation of KCNQ/M-channel modulators. *Assay Drug Dev Technol* 2006; 4: 49–56.

45. Wickenden AD, Krajewski JL, London B, et al. N-(6-Chloro-pyridin-3-yl)-3,4-difluoro-benzamide (ICA-27243): a novel, selective KCNQ2/Q3 potassium channel activator. *Mol Pharmacol* 2008; 73: 977–986. doi:10.1124/mol.107.043216.

46. Zhao J, Wei X-L, Jia Y-S, et al. Silencing of herg gene by shRNA inhibits SH-SY5Y cell growth in vitro and in vivo. *Eur J Pharmacol* 2008; 579: 50–57. doi:10.1016/j.ejphar.2007.10.008.

47. Faravelli L, Arcangeli A, Olivotto M, et al. A HERG-like K+ channel in rat F-Il DRG cell line: pharmacological identification and biophysical characterization. *J Physiol (Camb)* 1996; 496: 13–23.

48. Friederich P, Benzenberg D, Trellakis S, et al. Interaction of volatile anesthetics with human Kv channels in relation to clinical concentrations. *Anesthesiology (Hagerst)* 2001; 95: 954–958.

49. Zimmermann K, Lennerz JK, Hein A, et al. Transient receptor potential cation channel, subfamily C, member 5 (TRPC5) is a cold-transducer in the peripheral nervous system. *Proc Natl Acad Sci USA* 2011; 108: 18114–18119. doi:10.1073/pnas.1115387108.

50. Vriens J, Owsianik G, Hofmann T, et al. TRPM3 is a nociceptor channel involved in the detection of noxious heat. *Neuron* 2011; 70: 482–494. doi:10.1016/j.neuron.2011.02.051.

51. Jerman JC, Brough SJ, Prinjha R, et al. Characterization using FLIPR of rat vanilloid receptor (rVR1) pharmacology. *Br J Pharmacol* 2000; 130: 916–922.

52. Correll CC, Phelps PT, Anthes JC, et al. Cloning and pharmacological characterization of mouse TRPV1. *Neurosci Lett* 2004; 370: 55–60. doi:10.1016/j.neulet.2004.07.058.

53. Witte DG, Cassar SC, Masters JN, et al. Use of a fluorescent imaging plate reader–based calcium assay to assess pharmacological differences between the human and rat vanilloid receptor. *J Biomol Screen* 2002; 7: 466–475. doi:10.1177/108705702237679.

54. Darmanis S, Sloan SA, Zhang Y, et al. A survey of human brain transcriptome diversity at the single cell level. *Proc Natl Acad Sci USA* 2015; 112: 7285–7290. doi:10.1073/pnas.1507125112.

55. Madrid R, Edl Pena, Donovan-Rodriguez T, et al. Variable threshold of trigeminal cold-thermosensitive neurons is determined by a balance between TRPM8 and Kv1 potassium channels. *J Neurosci* 2009; 29: 3120–3131. doi:10.1523/JNEUROSCI.4778-08.2009.

56. Boland LM and Dingledine R. Expression of sensory neuron antigens by a dorsal root ganglion cell line, F-11. *Dev Brain Res* 1990; 51: 259–266.

57. Thakur M, Crow M, Richards N, et al. Defining the nociceptor transcriptome. *Front Mol Neurosci* 2014; 7: 87. doi:10.3389/fnmol.2014.00087.

58. Ranade SS, Woo S-H, Dubin AE, et al. Piezo2 is themajor transducer of mechanical forces for touch sensation inmice. *Nature (Lond)* 2014; 516: 121–125. doi:10.1038/nature13980.

59. Chiesa N, Rosati B, Arcangeli A, et al. A novel role for HERG K+ channels: spike-frequency adaptation. *J Physiol (Camb)* 1997; 501: 313–318.

60. Kovalevich J and Langford D. Considerations for the use of SH-SY5Y neuroblastoma cells in neurobiology. In: Amini S and White MK (eds) *Neuronal cell culture: methods and protocols. Methods in molecular biology.* New York: Humana Press, 2013.